Microbending effects on monomode light propagation in multimode fibers

F. de Fornel and J. Arnaud

Laboratoire d'Electronique des Microondes, Equipe de Recherche Associée au Centre National de la Recherche Scientifique No. 535, Limoges University, Limoges, France

P. Facq

Laboratoire d'Optique, Equipe de Recherche Associée au Centre National de la Recherche Scientifique No. 535, Limoges University, Limoges, France

Received April 23, 1982; revised manuscript received November 8, 1982

The effects of periodic axis deformations on propagation in multimode optical fibers with single-mode excitation are investigated numerically and experimentally. The numerical study, based on ray theory, deals with helical rays in the presence of sinusoidal axis deformations for various shapes of index profile. The corresponding experimental observations and results, carried out on tubular modes, confirm the existence of resonance effects between the helical ray period and the fiber axis deformation. This technique permits the observation of mode-to-mode power transfer and provides a sensitive tool to investigate the mode-coupling mechanism in optical fibers.

1. INTRODUCTION

Two of the most important transmission parameters in multimode optical fiber communications, namely, attenuation and bandwidth, are sensitive to microbends. Microbends induce mode mixing. As the optical power propagates along the fiber, leaky modes get coupled and some power is radiated. Thus mode mixing causes losses. Nevertheless it may have a favorable effect on bandwidth since it has a tendency to average the group delays of the various propagating modes.

The effect of microbends is often globally considered (with statistical models) since it results from the influence of complicated curvature distributions acting on numerous modal-field configurations. By spectral analysis, microbending can be viewed as the sum of periodic perturbations. Any field configuration in the fiber, on the other hand, can be considered as a sum of modal fields. Thus periodic perturbation of multimode fibers under single-mode operation provides an accurate tool for investigating the details of the coupling mechanism in multimode fibers.

In previous related work, Field[1] studied the effect of periodic microbending on losses for multimode fibers under Lambertian excitation. A strong resonance effect (high losses) was pointed out for square-law profile fibers when the microbend period equals the ray period $2\pi r_c/(2\Delta)^{1/2}$, where r_c denotes the core radius and Δ the maximum relative index difference. These effects are observed with fiber deformations whose amplitudes are of the order of a few micrometers.

In this paper we present a theoretical and experimental study of the effect of periodic microbends on multimode fiber propagation with single-mode excitation. The study has been carried out on fibers having various power-law and undulated index profiles. Numerical calculations based on ray theory show that helical ray propagation conditions strongly depend on the microbend period. Resonant effects give high losses whenever the microbend period matches the ray period (helix period). On the other hand, rays whose period does not match the fiber deformation period remain almost unperturbed as long as the deformation amplitude remains moderate. Experimental results on tubular-mode propagation (such modes are the wave-optics equivalent of helical rays) are found to be in good agreement with the theory. As predicted, resonance effects are observed whenever the period of the induced microbends fits the helical ray period. An experimental observation of nonadjacent mode coupling in undulated profile fibers is also presented.

2. NUMERICAL EVALUATION OF HELICAL RAY TRAJECTORIES IN A FIBER WITH SINUSOIDAL BENDS

The propagation of light in multimode fibers can usually be described by ray theory. (We limit ourselves to paraxial ray theory, which is sufficiently accurate when the fiber-index change is $\Delta \simeq 0.01$.) The ray trajectory can be obtained from the following equations[2,3]:

$$d^2x/dz^2 = -\partial U(x,y)/\partial x + C_x(z), \tag{1a}$$

$$d^2y/dz^2 = -\partial U(x,y)/\partial y + C_y(z), \tag{1b}$$

where $x = x(z)$; $y = y(z)$ describes the ray trajectory. $U(x, y)$ is related to the index profile $n(x, y)$ according to

$$U(x,y) = 1 - n(x,y)/n_0, \tag{2}$$

where $n_0 = n(0, 0)$ is the refractive index on axis; $C_x(z)$ and $C_y(z)$ are the fiber curvatures in the xz and yz planes. Equations (1) show that the curvature d^2x/dz^2 or d^2y/dz^2 of the ray trajectory is the sum of two terms. One is related to

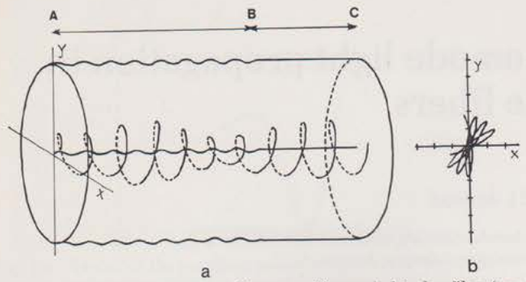

Fig. 1. a, Ray trajectory in a linear-profile graded-index fiber ($\kappa = 0.5$), subject to sinusoidal axis deformation, with amplitude $A_0 = 0.5$ μm in part AB. The ray is launched under such conditions that it would be helical in the absence of microbends. For clarity, the fiber representation has been compressed 30 times following the z axis. $r_c = 26$ μm, $\mu = 4$, $r_m = 5.1$ μm, N.A. = 0.25. b, Cross-section projection of the part of the ray traveling in the undeformed region BC following immediately the microbend region AB.

the refractive-index gradient $\partial U(x,y)/\partial x$ or $\partial U(x,y)/\partial y$, the other to the fiber axis curvature $C_x(z)$ or $C_y(z)$. From Eqs. (1a) and (1b), it is possible to calculate ray trajectories for various fiber-index profiles and various microbendings.

First let us consider helical trajectories in the absence of microbends. Helical rays are rays that remain at a constant distance r_m from the fiber axis. The geometrical parameters $x, y, \dot{x}, \dot{y}$ are related to the azimuthal mode number μ by[3]

$$\mu = k_0(x\dot{y} - y\dot{x}), \tag{3a}$$

where

$$\dot{x} = \mathrm{d}x/\mathrm{d}z, \qquad \dot{y} = \mathrm{d}y/\mathrm{d}z, \tag{3b}$$

and $k_0 = (\omega/c)n_0$, where $\omega = 2\pi f$ is the optical angular frequency. The complex amplitude of the field of tubular modes[4] has the following form in cylindrical coordinates r, ϕ, z:

$$\psi_\mu(r, \phi, z) = f(r)\cos \mu\phi \exp(i\beta z), \tag{4}$$

where $\psi_\mu(r, \phi, z)$ has no zero in the radial direction and whose radial dependence $f(r)$ has the appearance of a Gaussian curve centered at $r = r_m$. β is the propagation constant.

Next, let us assume that the fiber axis is deformed and described by an equation $x_d = A(z)$ in a rectangular xz coordinate system with

$$A(z) = A_0 \sin(2\pi z/\Lambda), \tag{5}$$

where A_0 is the deformation amplitude and Λ is the period. The corresponding curvature $C_x(z)$ is

$$C_x(z) = \mathrm{d}^2A(z)/\mathrm{d}z^2, \qquad C_y(z) = 0. \tag{6}$$

Thus

$$C_x(z) = -(4\pi^2\Lambda_0/\Lambda^2)\sin(2\pi z/\Lambda). \tag{7}$$

Once we have selected $C_x(z)$ and $U(x, y)$ in Eqs. (1a) and (1b), the trajectory can be determined by numerical integration, using Euler's method. In the absence of microbending, the ray projection in the xy plane is a circle. When microbends are present, the ray does not remain at a fixed distance from the axis (Figs. 1a and 1b). To simulate tubular-mode propagation we consider a ray congruence with μ and r_m constants. The initial conditions $(x_0, y_0, \dot{x}_0, \dot{y}_0)$ for the various rays are selected from the following relations:

$$x_0 = r_m \cos \gamma, \tag{8a}$$

$$y_0 = r_m \sin \gamma, \tag{8b}$$

$$\dot{x}_0 = R_d \sin \gamma, \tag{8c}$$

$$\dot{y}_0 = -R_d \cos \gamma, \tag{8d}$$

where γ is an angle that specifies one particular ray of the congruence and R_d is given by

$$R_d = -\mu/k_0 r_m. \tag{9}$$

The values of γ are taken as uniformly distributed between 0 and 2π. When microbends are applied, the ray projections in the xy plane are off-centered curves, the form of which depends on initial conditions. The rays no longer propagate at a constant distance from the fiber axis. In order to characterize the effect of microbending, let us define a thickness parameter w by

$$w = r_{\max} - r_{\min}, \tag{10}$$

where $r_{\max}$ and $r_{\min}$ are the maximum and minimum values

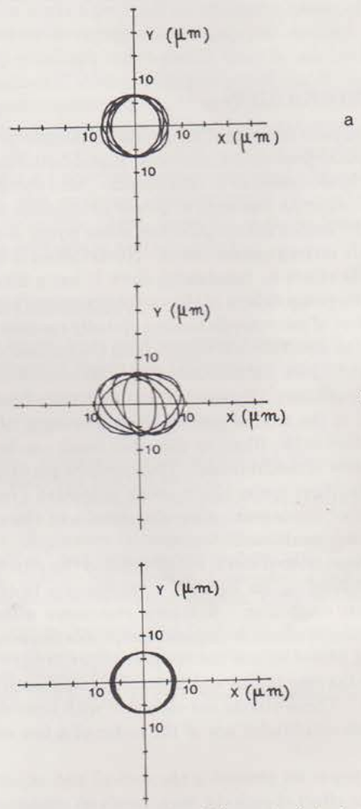

Fig. 2. Cross-section projection of the ray trajectories for different values of the perturbation-period to ray-period ratio Λ/p (with $A_0 = 5.10^{-3}$ μm, $\kappa = 1$, $\mu = 4$, $r_c = 26$ μm, $r_m = 6.4$ μm, $\gamma = m\pi/2$, and $m = 0, 1, 2, 3, 4$). a, $\Lambda/p = 0.5$; b, $\Lambda/p = 1$; c, $\Lambda/p = 1.5$.

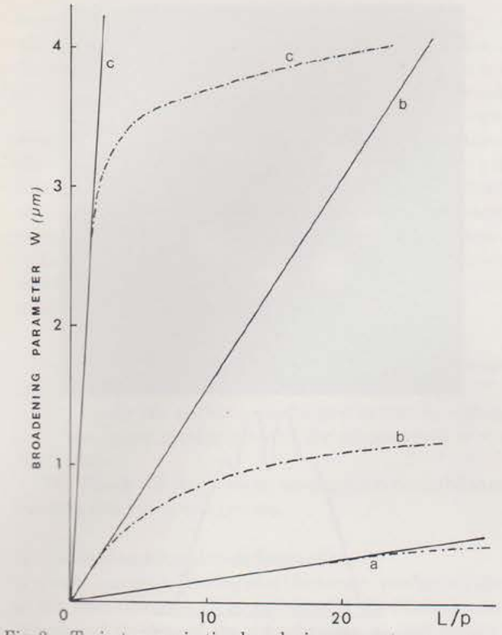

Fig. 3. Trajectory projection broadening parameter w versus perturbation-length to resonant-period ratio L/p for two index profiles: parabolic ($\kappa = 1$, $r_m = 6.4$ μm; solid line) and linear with $\mu = 4$ and $r_c = 26$ μm ($\kappa = 0.5$, $r_m = 5.1$ μm; dotted–dashed line), with various deformation amplitudes A_0: a, 1.25×10^{-3} μm; b, 1.25×10^{-2} μm; c, 1.25×10^{-1} μm.

of r, respectively, at the exit of the microbend region, for the various rays considered. If the applied microbending period Λ equals the period p of the helical ray trajectory, the w parameter reaches its maximum values (Fig. 2). We call this effect the resonance effect. Figure 3 gives the w variation as a function of the length L of fiber subjected to microbending. We can see from these figures that for a parabolic-index-profile fiber, w is proportional to the microbend fiber length L. For a constant value of $A_0 \times L$, w remains a constant.

Triangular-index-profile fibers exhibit quite a different behavior. If $A_0 \times L$ is small, w varies linearly with length L (Fig. 3), but if $A_0 \times L$ is longer, the curve shows a saturation effect. To explain this difference, one must recall that in parabolic-index-profile fibers, all the rays have the same period p. Thus the ray remains sensitive to further perturbations and the trajectory gets more and more deformed. In the triangular-index-profile fiber, however, the ray period is modified by the initial perturbation, and thus the rest of the ray trajectory is essentially unperturbed because of lack of synchronism.

3. TUBULAR-MODE LAUNCHING AND PROPAGATION

Using spatial-filtering techniques, Facq *et al.*[4] have shown that tubular-mode propagation (for $\mu = 4$) is possible in linear-profile fibers. We have verified that single-mode propagation succeeds as well for other kinds of index profiles and for various values of the azimuthal orders.

The tubular-mode radius r_m is the solution of

$$\mu^2/k_0^2 r_m^3 = \mathrm{d}U(r_m)/\mathrm{d}r_m, \tag{11}$$

provided that the potential function

$$U'(r) = U(r) + (1/2)(\mu/k_0 r)^2 \tag{12}$$

is minimum (rather than maximum) at $r = r_m$.

The tubular-mode filter used in the experiments is similar to the one described in Ref. 5. The field amplitude is synthesized in a binary manner. Whenever the field amplitude exceeds some fixed value, it is approximated by a constant value and otherwise by zero. A near plane wave is launched on a brass plate pierced by 2μ holes. This plate is held between two glass plates of optical quality in order to create 2μ cavities. The change in sign of the $\cos \mu\phi$ function in Eq. (4) is achieved by setting the air pressure at alternately low and atmospheric values in the holes. The resulting air-index variation provides the π phase shift required between rays traveling through adjacent cavities. After suitable scaling, the far-field pattern of the filter is launched into the fiber under test. The far-field pattern is almost identical to that of the near field behind the filter except for the scale factor, because Laguerre–Gauss fields are their own Fourier transforms. Figures 4a, 5a, 6a, and 7a show the near-field patterns at output ends of fibers with various index profiles for various values of the azimuthal number μ. All the fiber samples are 10 m long. Except for the last case (Fig. 7a), the tubular modes propagate without significant mode coupling. In the fiber with an undulated index profile, for a $\mu = 2$ tubular mode intended to be excited, we observe that the $\mu = 5$ tubular mode gets excited as well.

4. EXPERIMENTAL SETUP FOR OBSERVATION OF MICROBENDING EFFECT

A. Experimental Details and Procedure

The experimental apparatus used is the setup described for single-mode operation in multimode fibers,[5] completed by a device producing periodic mechanical action on the fiber. A spatial-filtering technique at the output end of the fiber provides a quantitative evaluation of the effects of microbending.

In order to induce periodic microbends, the fiber is pressed between two identical circular plates engraved with equally spaced parallel grooves (period Λ_0). Variation of the perturbation period Λ is obtained by giving the fiber axis an angle α with respect to the normal to the grooves (Fig. 8); thus

$$\Lambda = \Lambda_0/\cos \alpha. \tag{13}$$

Two sets of grooved aluminum plates have been machined with a saw-toothed profile, with fundamental period Λ_0 equal to 0.5 and 0.7 mm, respectively. The plate diameter is 100 mm. To avoid breaking the fiber, the tooth edges have been smoothed by light polishing.

A quantitative estimate of the effect of microbending on tubular-mode propagation is obtained as follows. In the absence of perturbation the tubular-mode power flows through a limited area of the core: a ring whose mean radius r_m is an increasing function of the azimuthal order μ of the mode.[4] Under periodic bending of the fiber, the light power is trans-

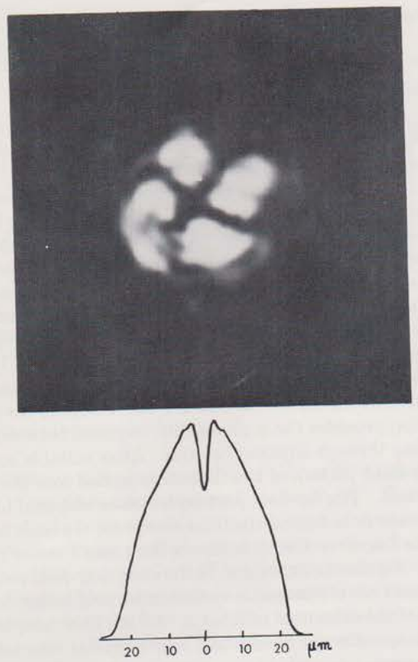

Fig. 4. a, $\mu = 2$ tubular mode at the output end of a 10-m-long quadratic-index profile fiber. $r_m = 4\ \mu$m. b, Index profile of the corresponding fiber ($r_c = 26\ \mu$m, N.A. = 0.25).

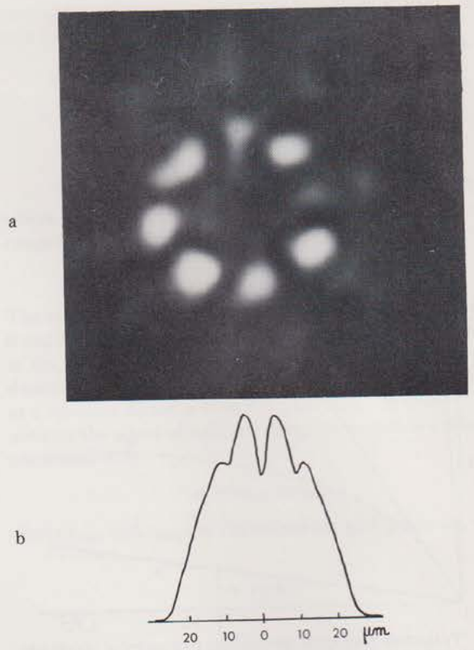

Fig. 6. a, $\mu = 4$ tubular mode at the output end of a 10-m-long fiber, $r_m = 5.5\ \mu$m. b, Index profile of the corresponding fiber ($r_c = 26\ \mu$m, N.A. = 0.17).

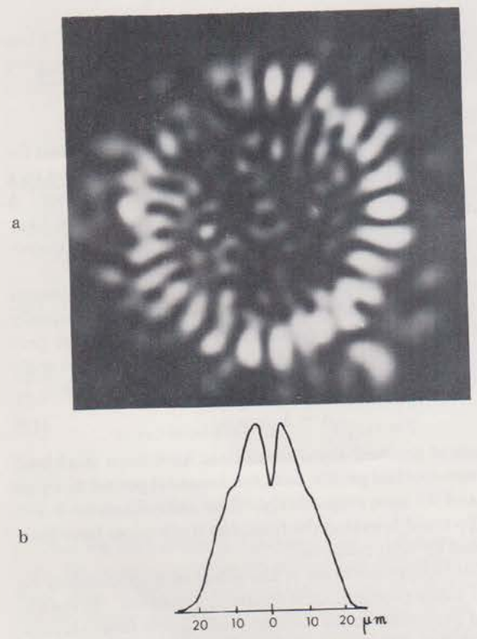

Fig. 5. a, $\mu = 13$ tubular mode at the output end of a 10-m-long linear-profile fiber $r_m = 10.5\ \mu$m. b, Index profile of the corresponding fiber ($r_c = 21\ \mu$m, N.A. = 0.21).

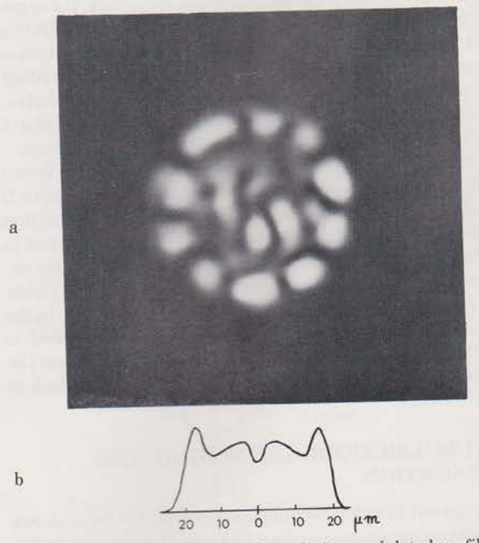

Fig. 7. a, Photograph of the exit end of an undulated profile fiber showing the appearance of a $\mu = 5$ tubular mode at r_m 16.4 μm when a $\mu = 2$ tubular mode has been launched at $r_m = 4.6\ \mu$m. b, Undulating index profile of the fiber ($r_c = 24\ \mu$m, N.A. = 0.11).

ferred to other modes, in particular to higher-order modes, whose power is located at larger distances from the fiber axis. To isolate the amount of power coupled to higher-order modes $\mu' > \mu$, we block the launched tubular-mode power by masking the central area of the output near-field pattern with a circular screen of radius r_s (Fig. 9). The power P_{ext} flowing through the remaining annular area $r_s < r < r_c$ is received on a photodetector. Visual observation and photographic recording of the near field at the output end of the fiber give complementary information about the propagation conditions.

To verify the injection-condition stability, each measurement at a given value Λ of the induced microbend period is made according to the following procedure:

(1) Check for single-mode propagation in the absence of induced microbend (upper grating removed).
(2) Apply the periodic mechanical action by setting in place the upper grating plate at the proper angle $\alpha = \arccos(\Lambda_0/\Lambda)$.
(3) Check for single-mode propagation reestablishment by removing the upper grating.

B. Microbend Amplitude Estimation

If we assume the following ideal features: perfect regularity of the fiber diameter D, straightness of the fiber axis before stress, and flatness of the ridged plates, we can deduce the fiber-axis distortion amplitude $\bar{a}$ from the laws of linear elasticity, where F is the upper grating weight and E is the Young modulus of silica; thus we have

$$\bar{a} = F\Lambda^4/(3\pi EID^4), \tag{14}$$

with $E = 7 \times 10^{10}$ N/m^2, $F = 1$ N, $\Lambda = 0.5$ mm, $l = 100$ mm, $D = 125\ \mu$m; Eq. (14) gives

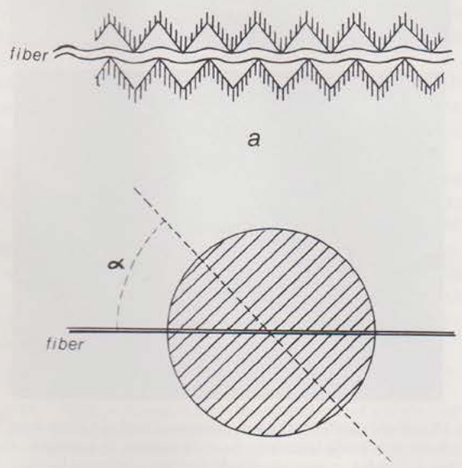

Fig. 8. Fiber-deformation device. a, Side view; b, top view.

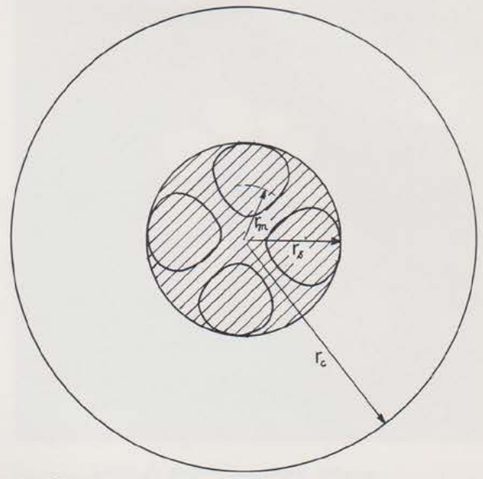

Fig. 9. Circular mask for $\mu = 2$ tubular-mode blockage. The power flowing through the area $r_s < r < r_c$ is collected by a photodetector.

$$\bar{a} = 4 \times 10^{-3}\ \mu\text{m}.$$

We note the very small deformation amplitude, which is nevertheless sufficient to cause severe effects on the tubular-mode propagation. Such an amplitude is much smaller than the tolerance over fiber diameter and grating-plate flatness. Therefore the mechanical stress most likely is not evenly distributed, and the local distortion amplitude may depart from the value $\bar{a}$ given in Eq. (14). Nevertheless $\bar{a}$ can be interpreted as a mean value of the distortion amplitude over the grating length.

5. EXPERIMENTAL RESULTS

Tubular-mode launching and periodic microbends have been applied to multimode fibers having various refractive-index profiles: square-law profiles, linear profiles, and various kinds of undulated profiles. The experiments are made with He–Ne laser light ($\lambda = 0.633\ \mu$m). The fiber-core diameters are $2r_c = 50\ \mu$m.

A. Parabolic-Index-Profile Fiber

A tubular mode of azimuthal order $\mu = 2$ has been launched into a square-law chemical-vapor-deposition fiber and periodic microbends applied with variable period Λ. Figures 10 and 11 are sketches of the power P_{ext} versus Λ for two different values of the force F. We note the sharp resonant behavior of p_{ext} at $\Lambda = 1{,}17$ mm that is near the theoretical period p of helical rays in that square-law fiber: $p = 1$ mm for all μ values. In square-law-profile fibers all the propagating modes are thus perturbed. The propagation losses are strong at the resonant period.[1] The photographs in Fig. 12 show the near-field pattern at the output end of the fiber; in Fig. 12b the resonant case $\Lambda = 1$ mm is shown. Thus the speckle pattern spreads on the entire core area, giving the scale of the

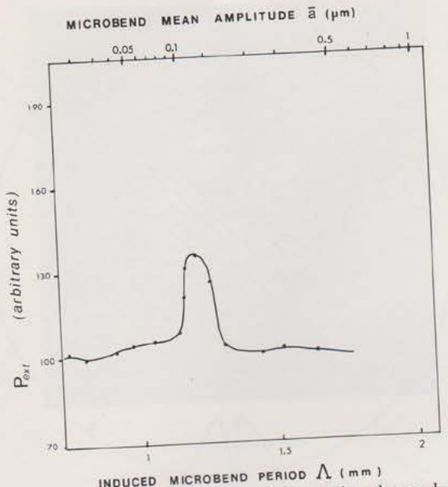

Fig. 10. Amount of power P_{ext} coupled to high-order modes and flowing outside the blocking screen of Fig. 9. Quadratic-index-profile fiber (see Fig. 4b) under $\mu = 2$ tubular-mode injection subject to periodic microbends of period Λ and mean amplitude $\bar{a}$. Total deformation force $F = 0.1$ N.

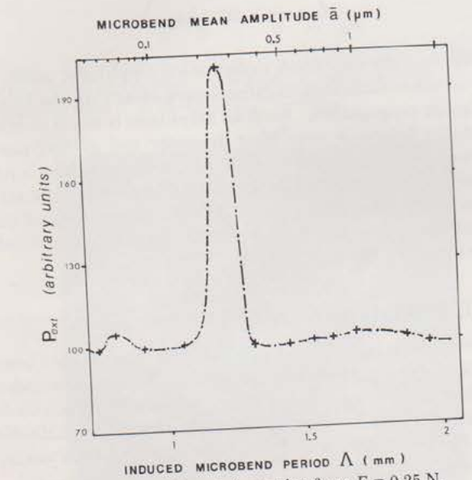

Fig. 11. As in Fig. 10 for a deformation force $F = 0.25$ N.

fiber core. The small size of the speckle grains and their spatial distribution over the core show that most of the propagating modes have been coupled. For the $\mu = 4$ tubular mode, the resonance, as expected, is observed for $\Lambda = 1$ mm.

B. Linear-Index-Profile Fiber

For this fiber, whose index profile is sketched in Fig. 5b, the numerical aperture at $\lambda = 633$ nm is N.A. = 0.21. The calculated ray period for $\mu = 4$ is $p = 0.4$ mm, which is less than the basic period Λ_0 of the grating (0.5 mm). Nevertheless a weak resonance effect is observed with $\Lambda = 0.79$ mm, which is at about twice the ray period.

C. Weakly Undulating Index-Profile Fibers

The fiber under test has the index profile shown in Fig. 6. For that fiber, whose numerical aperture is N.A. = 0.17, a $\mu = 2$ tubular mode has a period $p = 1.05$ mm. A plot of P_{ext} versus Λ exhibits a weak resonance at $\Lambda = 0.98$ mm (Fig. 13). At this period P_{ext} is shifted by less than 8% of its value at nonresonant periods. Note that the relative increase of P_{ext} was 40% at the resonant period for a square-law-profile fiber under the same perturbation conditions. We observe (at the resonant

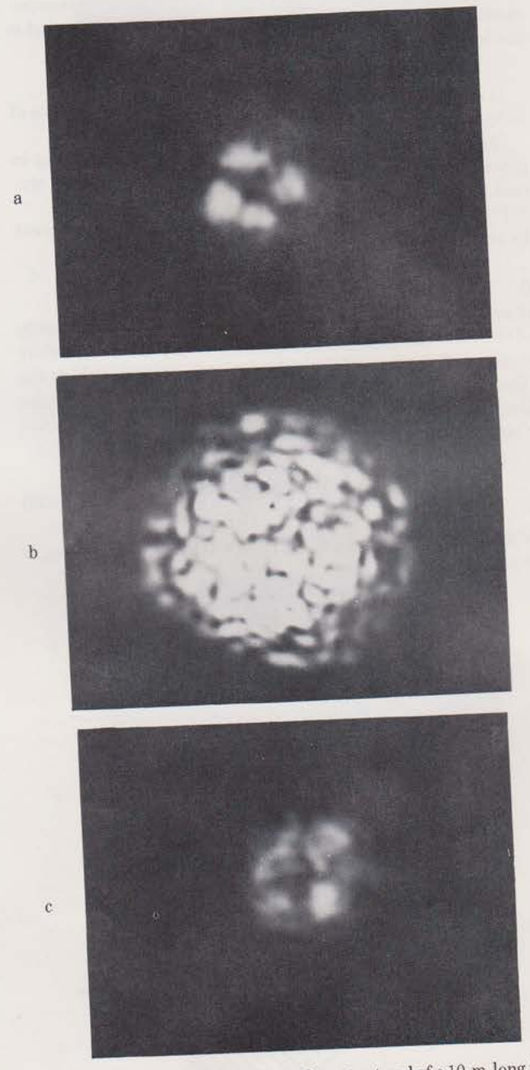

Fig. 12. Field configurations at the output end of a 10-m-long fiber under tubular-mode launching ($\mu = 2$), subject to a periodic deformation (period Λ, mean amplitude $\bar{a}$) over a 100-mm length. The $\mu = 2$ ray period in that quadratic-index-profile fiber is $p = 1$ mm. $F = 0.25$ N. a, $\Lambda/p = 0.6$, $\bar{a} = 10^{-2}$ μm; b, $\Lambda/p = 1$, $\bar{a} \simeq 0.1$ μm; c, $\Lambda/p = 1.2$, $\bar{a} \simeq 0.25$ μm.

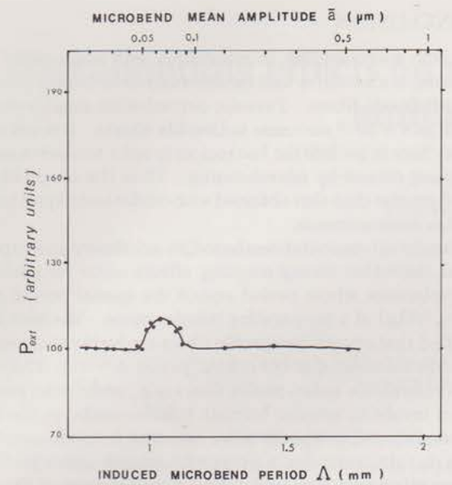

Fig. 13. Amount of power P_{ext} coupled to high-order modes and flowing outside the blocking screen of Fig. 9. Slightly undulating index-profile fiber (see Fig. 6b) under $\mu = 2$ tubular-mode launching, subject to periodic microbends of period Λ and mean amplitude $\bar{a}$.

period $\Lambda = 0.98$ mm) that the tubular mode $\mu = 2$ is weakly perturbed. The mode pattern suffers slight distortions but remains in the vicinity of the $\mu = 2$ mode area, showing that the light power apparently couples to adjacent modes only. In such undulated-profile fibers, tubular modes appear to be resistant to mode mixing. This property seems to be a consequence of a trapping effect in the index-profile bumps (Fig. 6b). It is also observed in Fig. 14, which gives, for the same fiber, the effect of periodic microbends on a $\mu = 4$ tubular mode whose resonance period is $\Lambda = 0.73$ mm ($p = 0.69$ mm).

D. Strongly Undulating Index-Profile Fibers

With strongly undulating index-profile fibers, selective power transfer can occur between nonadjacent tubular modes. Figure 7a shows an example in which a $\mu = 2$ tubular mode is launched into such a fiber, giving rise to $\mu = 2$ and $\mu = 5$ tubular-mode propagation. The index profile of the fiber is given in Fig. 7b. Figure 15 shows that the associated potential function $U'(r)$ given by Eq. (12) exhibits for $\mu = 2$ two minima in the range $0 < r < r_c$.

If the $\mu = 2$ tubular mode is launched in the fiber, the $\mu = 5$ tubular mode appears rapidly by mode coupling at radius $r_m = 16.4$ μm. The periods of those modes are $p = 0.96$ mm for $\mu = 2$ ($r_m = 4.6$ μm) and $p = 2.4$ mm for $\mu = 5$ ($r_m = 16.4$ μm), respectively. When the fiber is subject to microbends with $\Lambda = 0.96$ mm, the $\mu = 2$ tubular-mode propagation is perturbed, while the $\mu = 5$ tubular mode is not (see Fig. 16).

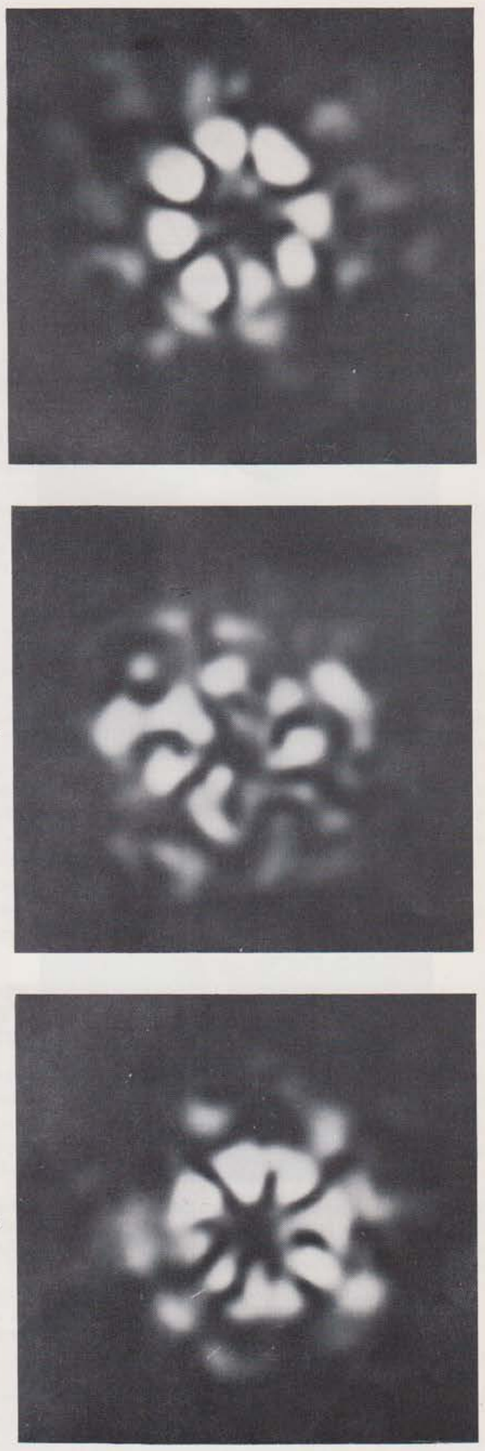

Fig. 14. Field configurations at the output end of a 10-m-long fiber under tubular-mode launching ($\mu = 4$) subject to a periodic deformation (period Λ) over a 100-mm length. The $\mu = 4$ ray period in that slightly undulating index profile is $p = 0.69$ mm. a, $\Lambda/p = 0.70$, $\bar{a} \simeq 1 \times 10^{-2}$ μm; b, $\Lambda/p = 1.06$, $\bar{a} \simeq 1.5 \times 10^{-2}$ μm; c, $\Lambda/p = 2.57$, $\bar{a} \simeq 0.6$ μm.

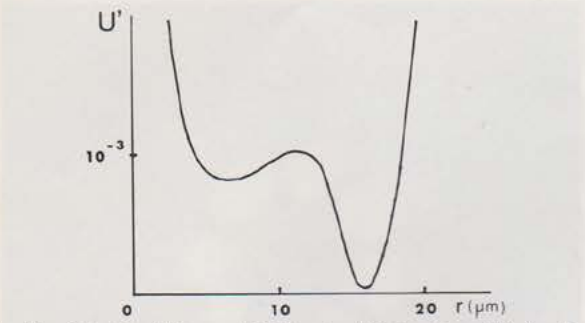

Fig. 15. Sketch of the modified potential function $U'(r) = [n_0 - n(r)]/n_0 + (1/2)(\mu/k_0 r)^2$ for $\mu = 2$ for the strongly undulating index profile of Fig. 7b.

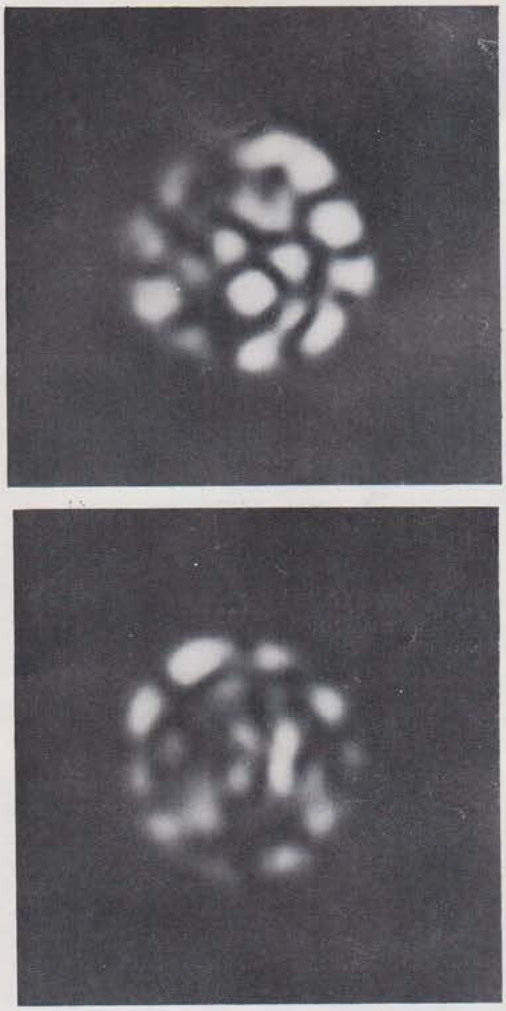

a

b

Fig. 16. Field configurations at the output end of a 10-m-long fiber under tubular-mode launching ($\mu = 2$) subject to a periodic deformation (period Λ) ($\bar{a} = 0.1\ \mu$m) over a 100-mm length. The $\mu = 2$ ray period in that strongly undulating index profile is $p = 0.96$ mm: a, $\Lambda/p \neq 1$; b, $\Lambda/p = 1$.

CONCLUSION

Periodic microbending, in association with single-mode excitation, is a sensitive tool for the analysis of mode coupling in multimode fibers. Periodic perturbation amplitudes as small as $4 \times 10^{-3}\ \mu$m cause noticeable effects. It is not necessary here to get into the loss regime in order to observe mode coupling caused by microbending. Thus the sensitivity is much greater than that obtained with cruder techniques based on loss measurements.

Numerical computations based on ray theory and experiment show that strong coupling effects occur for periodic perturbations whose period equals the spatial period $p = 4\pi^2 r_m{}^2/(\lambda\mu)$ of a propagating tubular mode. We have also verified that square-law-profile fibers are highly sensitive to periodic microbend at the critical period $\Lambda = 2\pi r_c/(2\Delta)^{1/2}$.[1] In nonparabolic-index-profile fibers (e.g., undulating profile fibers involving annular bumps), tubular modes at the corresponding radius appear more resistant to mode coupling than do tubular modes in fibers with smooth-index profiles. These effects are well understood with the help of the ray formalism. This formalism is quite convenient to describe the behavior of multimode fibers under single-mode excitation.

Let us now make a proposal for characterization of a fiber profile based on the experimental results just reported. When a nominally quadratic index-profile fiber is operated under tubular-mode excitation and its axis is periodically bent, the amount of power taken from the launched mode, together with the resonance sharpness, might be used as a criterion to decide how well the fiber's index profile fits a parabolic law. Whether this is a practical method remains to be shown.

One can also envisage selective mode extraction from nonparabolic-profile fibers, provided that the various ray periods are sufficiently well separated.

ACKNOWLEDGMENT

The fibers tested were kindly supplied to us by the French Centre National d'Etude des Télécommunications.

REFERENCES

1. J. N. Fields, "Attenuation of a parabolic index fiber with periodic bends," Appl. Phys. Lett. **36**, 10 (1980).
2. J. Arnaud and M. Rousseau, "Ray theory of randomly bent multimode optical fibers," Opt. Lett. **3**, 63–65 (1978).
3. J. Arnaud, "Application des techniques Hamiltoniennes aux fibres multimodales," Ann. Télécom. **32**, 135–143 (1977).
4. P. Facq, P. Fournet, and J. Arnaud, "Observation of tubular modes in multimode graded-index optical fibers," Electron. Lett. **16**, 648 (1980).
5. P. Facq and J. Arnaud, "Tubular mode excitation in graded-index multimode fibers" in *Proceedings of Photon 80, Quartz et Silice* (Pithiviers, France, 1980).
6. J. Arnaud, *Beam and Fiber Optics* (Academic, New York, 1976).